Mineral detectors on the moon

based on "The Final Frontier for Proton Decay" arXiv:2405.15845
with Sebastian Baum, Cassandra Little, Paola Sala and Joshua Spitz

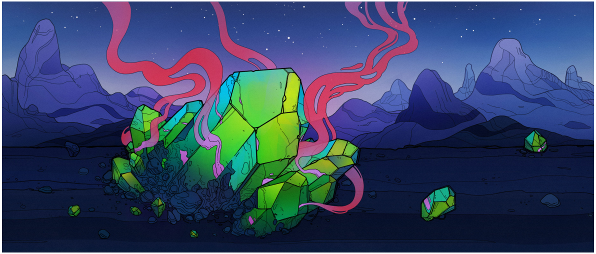

Figure: Olena Shmahalo/Quanta Magazine

Jožef Stefan Institute
Ljubljana, Slovenia

SMASH
machine learning for science and humanities postdoctoral program

Co-funded by the European Union

This project has received funding from the European Union's Horizon Europe research and innovation programme under the Marie Skłodowska-Curie grant agreement No. 101081355.

Mineral Detection of Neutrinos and Dark Matter May 20-23, 2025 at JAMSTEC in Yokohama, Japan

MDνDM'25 indico

Confirmed Speakers	Kohta Murase
Alexey Elykov	Lorenzo Caccianiga
Atsuhiro Umemoto	Noriko Hasebe
Ayuki Kamada	Patrick Huber
Christopher Kelso	Patrick Stengel
Christian Wittweg	Shigenobu Hirose
Daniel Ang	Takenori Kato
Daniel Snowden-Ifft	Tatsuhiro Naka
Emilie LaVoie-Ingram	Vsevolod Ivanov
Igor Jovanovic	William McDonough

Previous MDνDM workshops:

1. Trieste 2022
2. Arlington 2024

Damage features from recoils in ancient minerals

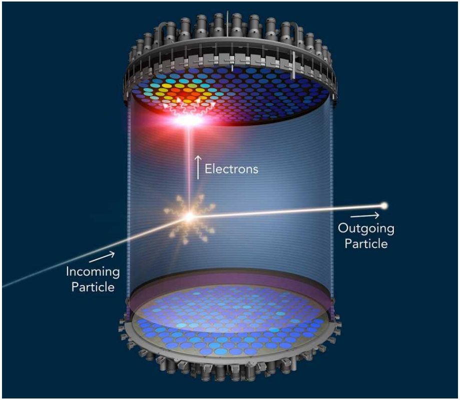

Figure: LUX-ZEPLIN (LZ) Collaboration / SLAC National Accelerator Laboratory

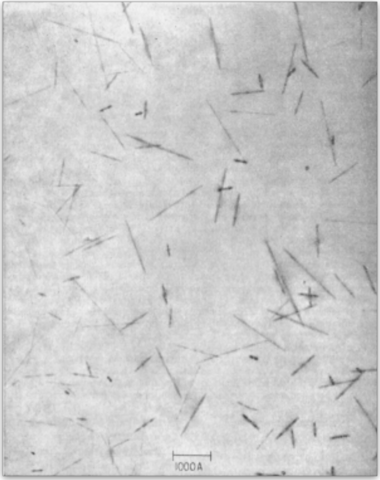

Figure: Price+Walker (1963)

Needle in a haystack

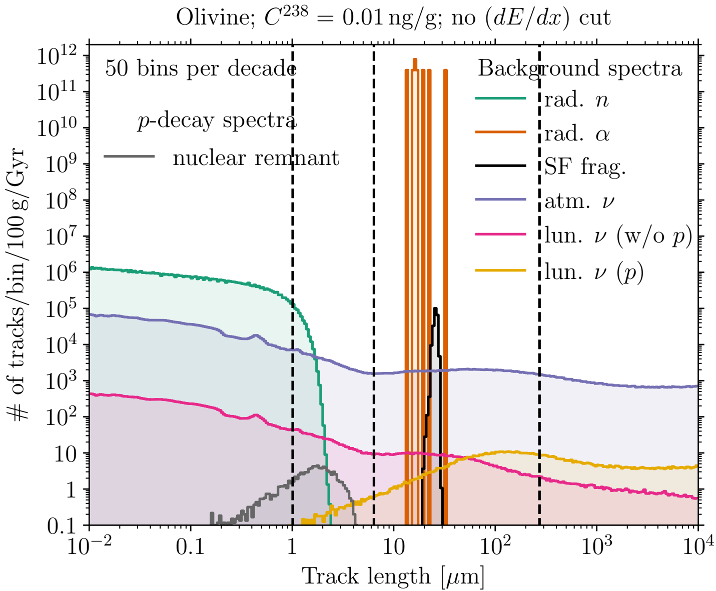

Large exposure from small target ⇒ $\mathrm{kg\,Gyr} = 1\,\mathrm{Mton\,yr}$

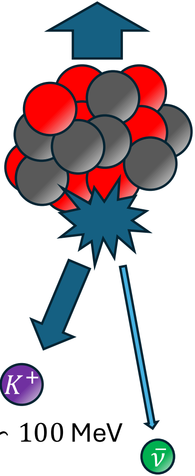

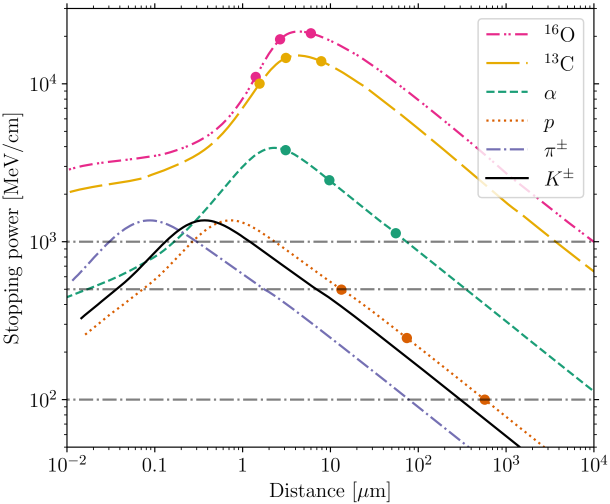

Fluorescent nuclear track detectors for K^+ endpoints

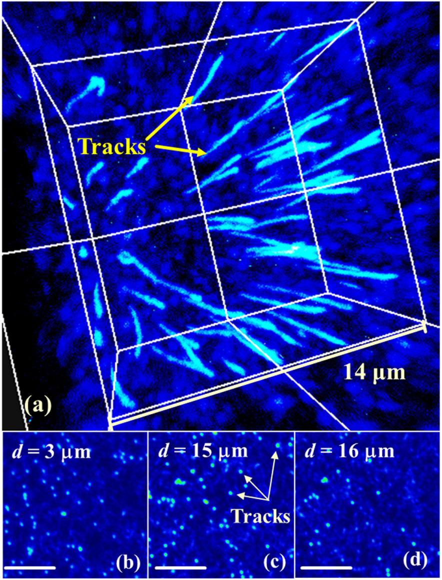

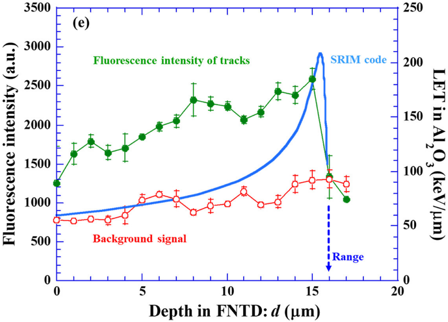

Figures from Kusumoto et al. (2022) show proton tracks in doped sapphire

- Theory of track formation?
- Are tracks robust to annealing?
- Use ***dE*/*dx* proxy** for tracks

Nuclear recoils from α-decays and spontaneous fission

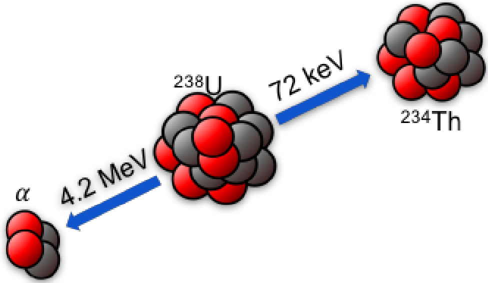

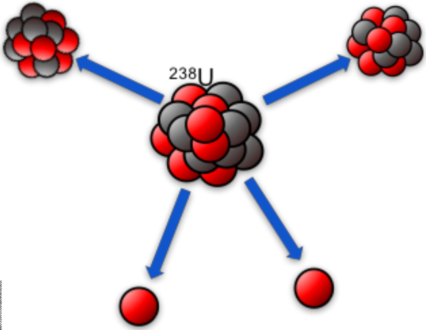

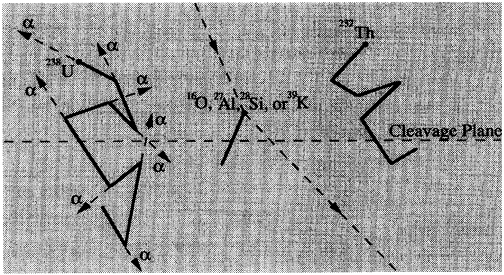

Need very radiopure minerals

Ultra-basic rocks formed in the mantle with $C^{238} \gtrsim 0.01\,\mathrm{ppb}$

Atmospheric neutrinos induce $\mathcal{O}(100)\ K^+/100\,\mathrm{g}/\mathrm{Gyr}$

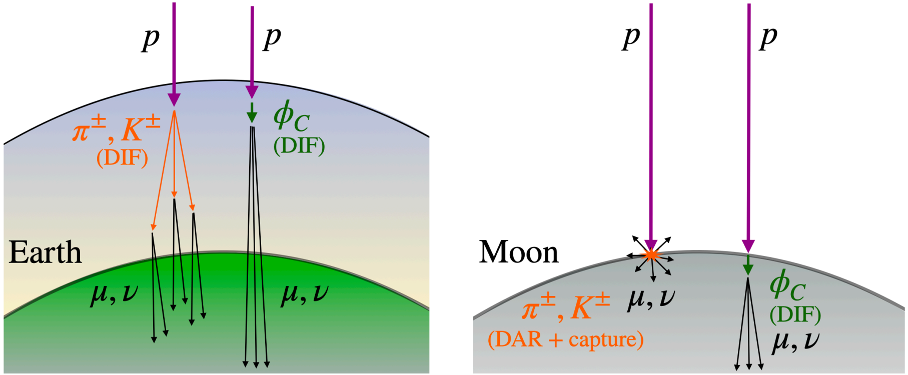

Figures from arXiv:2411.09634

- Conventional secondary mesons **decay in flight** on Earth
- Prompt fluxes from short-lived mesons decaying in flight

Suppression of lunar μ and ν fluxes

- Conventional secondary mesons **decay at rest** on the Moon
- Less suppression of short-lived mesons decaying in flight

Lunar neutrinos induce $\sim 0.5\, K^+/100\,\mathrm{g}/\mathrm{Gyr}$ in Olivine

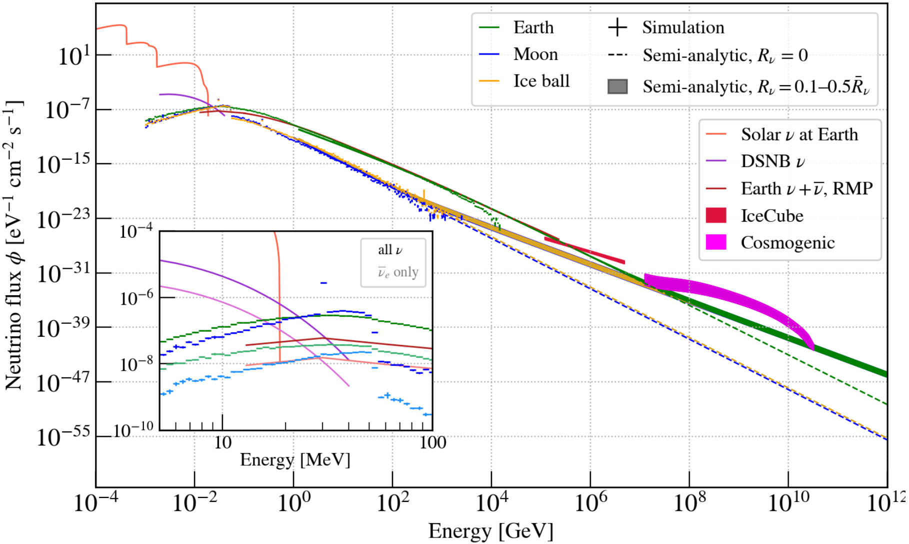

Lunar muons induce $\sim 0.1\, K^+/100\,\text{g}/\text{Gyr}$ at $\sim 5\,\text{km}$ depth

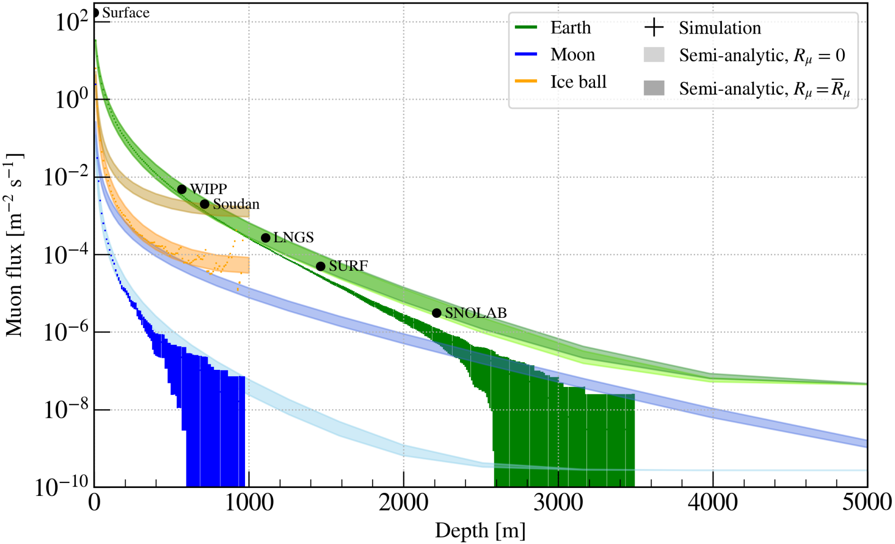

Expect $\lesssim 6\,K^+/100\,\mathrm{g}/\mathrm{Gyr}$ for $\tau(p \to \bar{\nu}K^+) > 5.9 \times 10^{33}$ yr

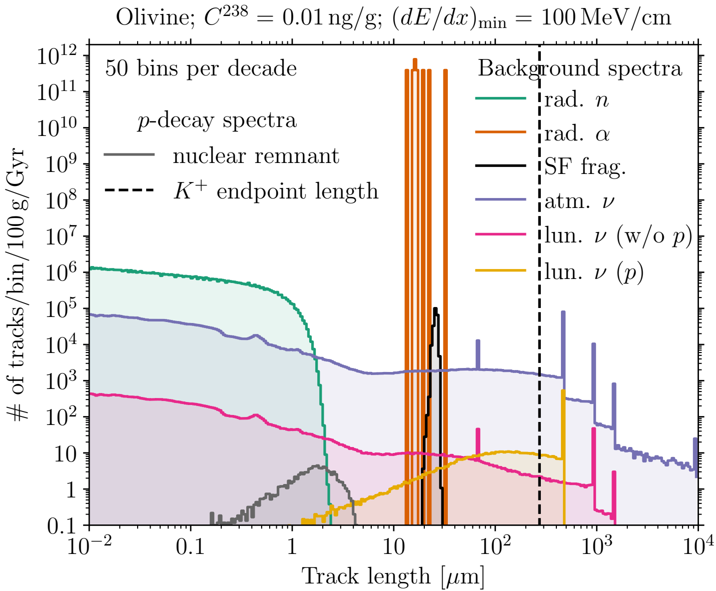

Increase dE/dx threshold from 100 to 500 MeV/cm

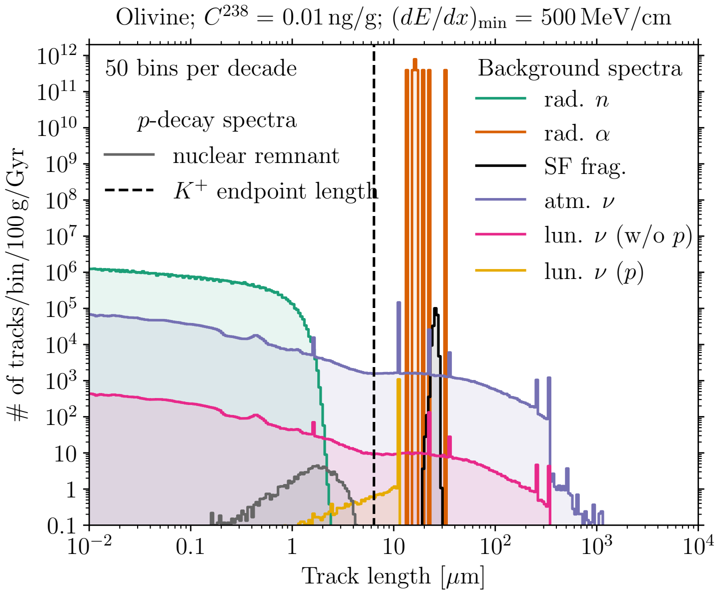

Large exposures in MDs could probe DM and proton decay

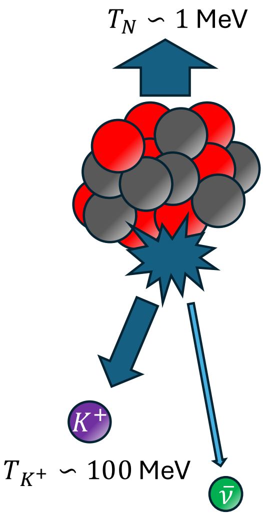

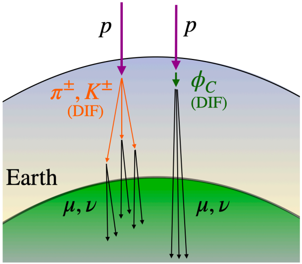

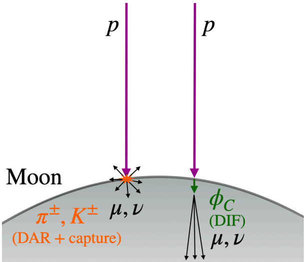

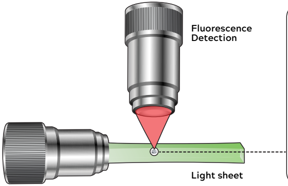

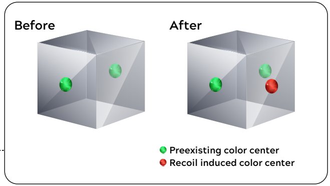

New techniques allow for much larger readout capacity

Irradiation dose is 80 ions per field of view (20umx20um).

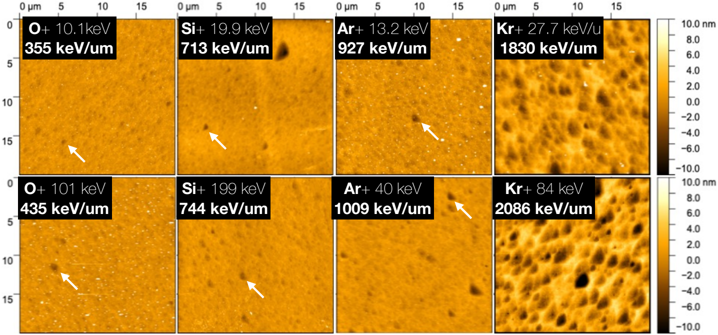

proxy	DM scattering	alpha recoils
pit formation efficiency	several to 10 %	~ 100%

Cleaving and etching limits ϵ and can only reconstruct 2D

Readout scenarios for different x_T

- HIBM+pulsed laser could read out 10 mg with nm resolution
- SAXs at a synchrotron could resolve 15 nm in 3D for 100 g

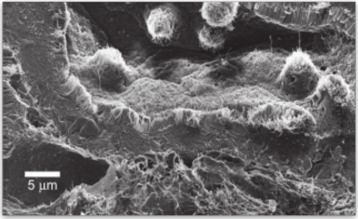

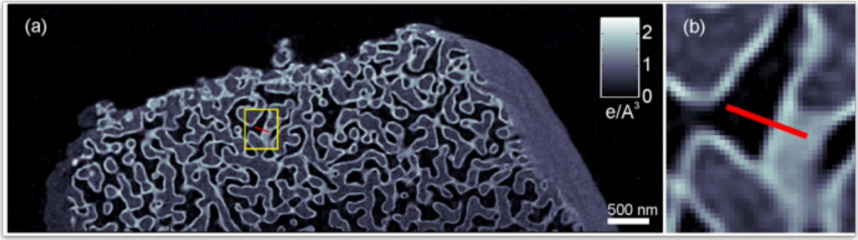

Figure: HIM rodent kidney Hill+ '12, SAXs nanoporous glass Holler+ '14

Integrate stopping power to estimate track length

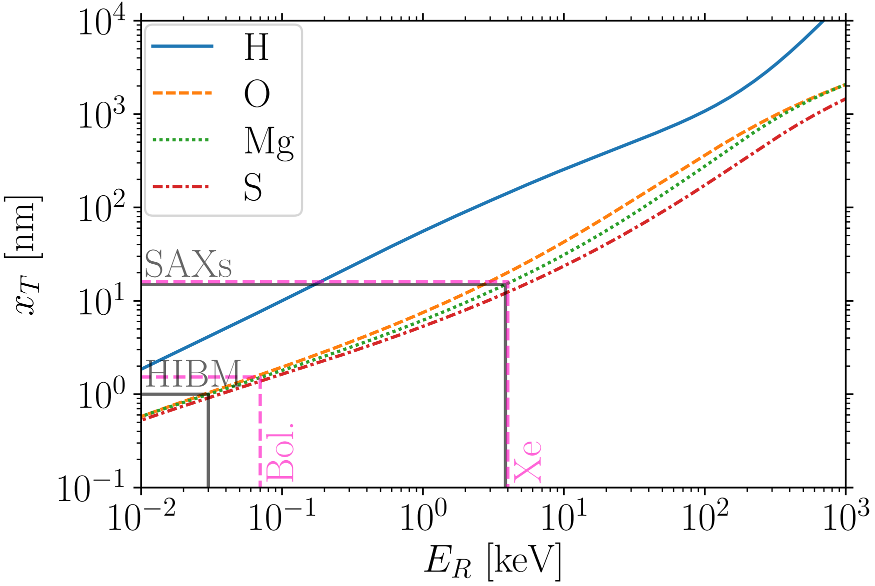

Recognition of sparse tracks is a data analysis challenge

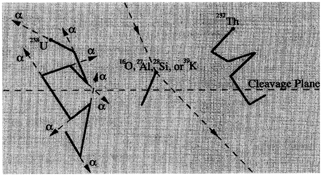

- 15 nm resolution of 100 g sample
  $\Rightarrow 10^{19}$ mostly empty voxels
- 1 Gyr old with $C^{238} = 0.01$ ppb
  $\Rightarrow 10^{13}$ voxels for α-recoil tracks

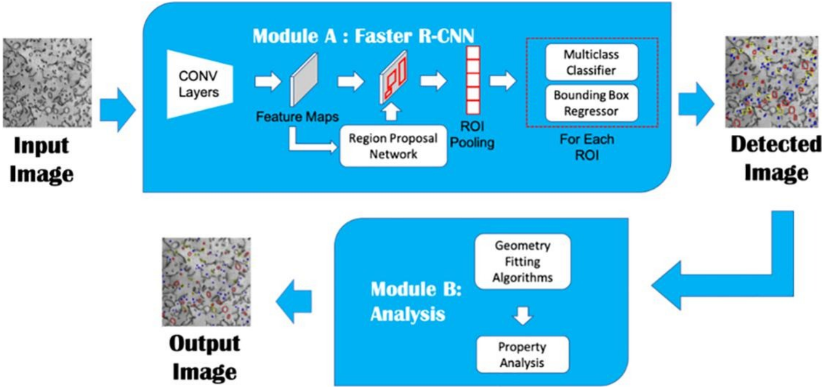

Scattering cross sections ⇒ scattering rates

$$\frac{d^2\sigma}{dq^2 d\Omega_q} = \frac{d\sigma}{dq^2}\frac{1}{2\pi}\delta\left(\cos\theta - \frac{q}{2\mu_{XT} v}\right) \simeq \frac{\sigma_0 F(q)^2}{8\pi\mu_{XT}^2 v}\delta\left(v\cos\theta - \frac{q}{2\mu_{XT}}\right)$$

$$\frac{d^2 R}{dE_R d\Omega_q} = 2M_T \frac{N_T}{M_T N_T}\int \frac{d^2\sigma}{dq^2 d\Omega_q} n_X\, v\, f(\boldsymbol{v}) d^3 v \simeq \frac{\sigma_0 F(q)^2}{4\pi\mu_{XT}} n_X \hat{f}(v_q, \hat{\boldsymbol{q}})$$

Differential cross section

- δ-function imposes kinematics
- σ_0 is velocity and momentum independent cross section for scattering off pointlike nucleus

$$F(q) \simeq \frac{9\left[\sin(qR) - qR\cos(qR)\right]^2}{(qR)^6}$$

Differential scattering rate

- Rate per unit time per unit detector mass for all nuclei
- Convolute cross section with astrophysical WIMP flux

$$\sigma_0^{SI} = \frac{4}{\pi}\mu_{XT}^2\left[Zf_s^p + (A-Z)f_s^n\right]^2$$

Nuclear recoils induced by elastic WIMP-nucleus scattering

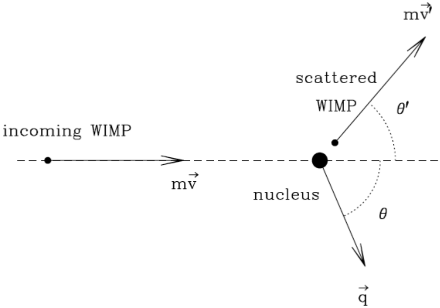

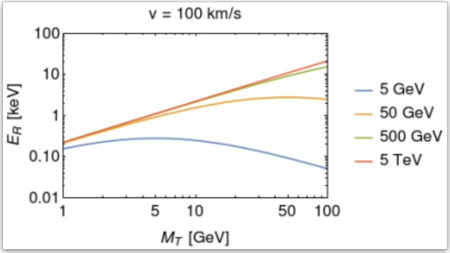

Scattering kinematics ⇒ event rate

- Account for finite size of nucleus
- Convolute with WIMP flux
- Write cross section in terms of WIMP-nucleon interaction

Rate per unit time per unit mass

$$\frac{dR}{dE_R} = \frac{n_X}{2} \frac{\sigma_{Xp}^{SI}}{\mu_{Xp}^2} A^2 F(q)^2 \eta(v_q)$$

WIMP velocity distribution and induced recoil spectra

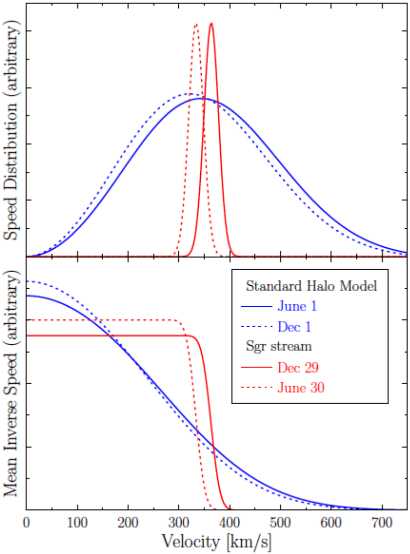

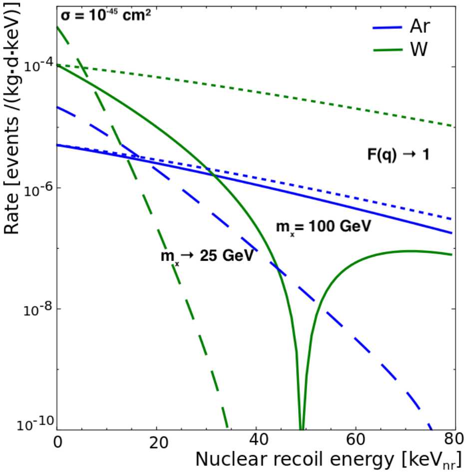

Figure: (left) 1209.3339 (right) 1509.08767

Mineral detectors used to constrain WIMPs before

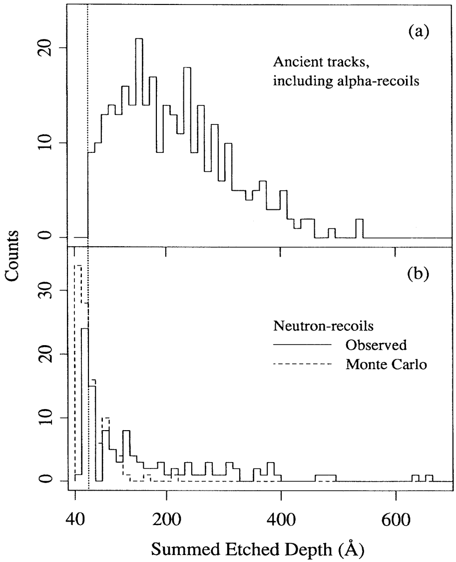

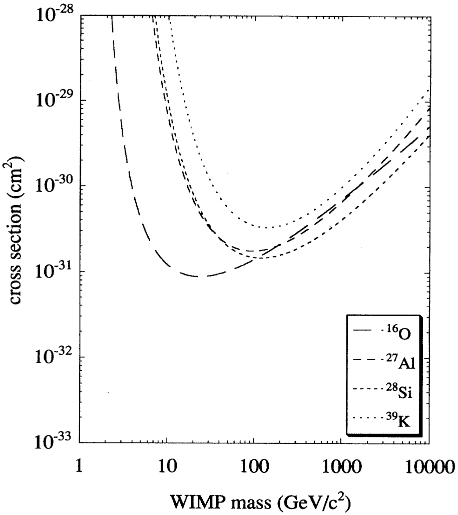

Figure: Snowden-Ifft et al. (1995)

Use track length spectra to pick out WIMP signal

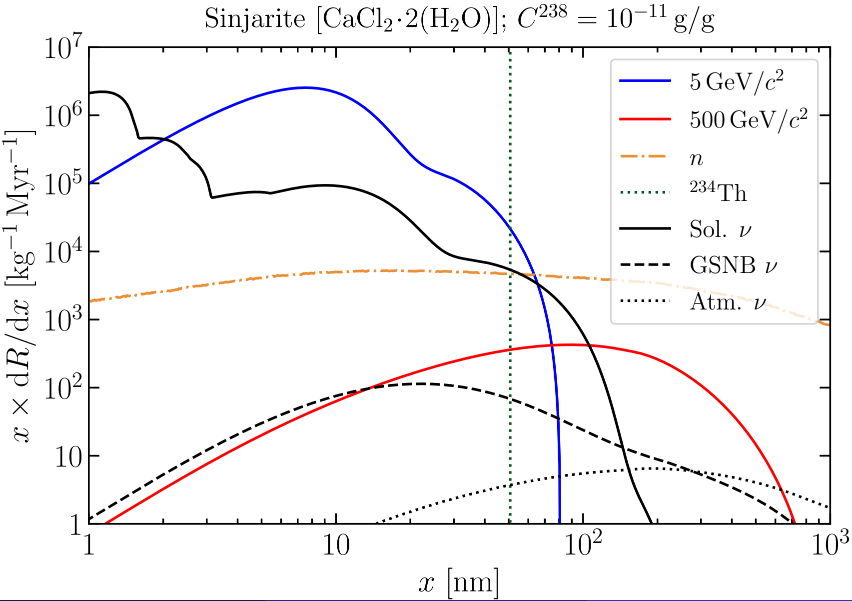

Track length spectra after smearing by readout resolution

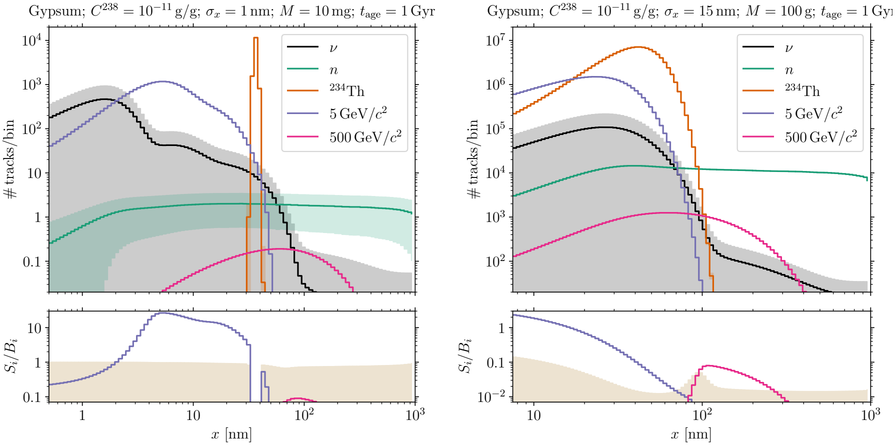

Trade-off between read-out resolution and exposure

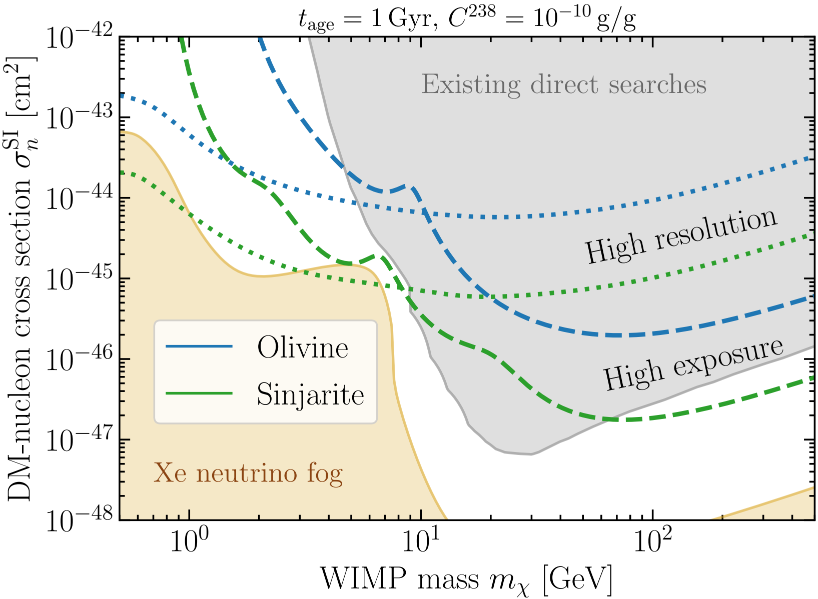

Sensitivity for different targets

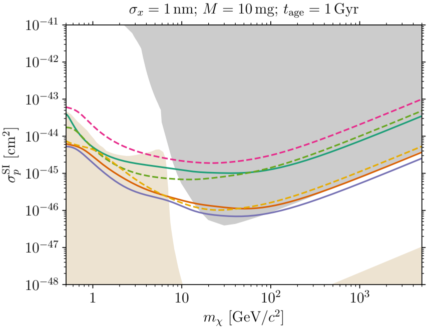

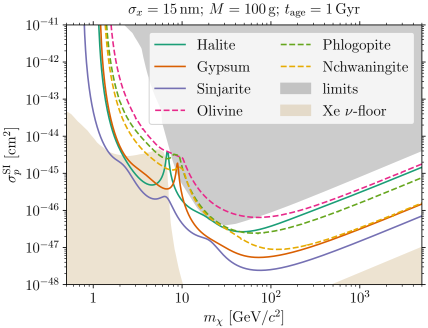

Halite	$NaCl$	$C^{238} = 10^{-11}$ g/g
Gypsum	$Ca(SO_4){\cdot}2(H_2O)$	$C^{238} = 10^{-11}$ g/g
Sinjarite	$CaCl_2{\cdot}2(H_2O)$	$C^{238} = 10^{-11}$ g/g
Olivine	$Mg_{1.6}Fe^{2+}_{0.4}(SiO_4)$	$C^{238} = 10^{-10}$ g/g
Phlogopite	$KMg_3AlSi_3O_{10}F(OH)$	$C^{238} = 10^{-10}$ g/g
Nchwaningite	$Mn^{2+}_2SiO_3(OH)_2{\cdot}(H_2O)$	$C^{238} = 10^{-10}$ g/g

Effects of background shape systematics

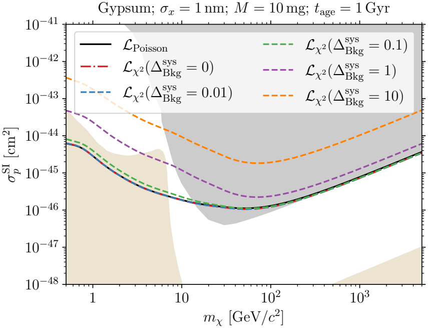

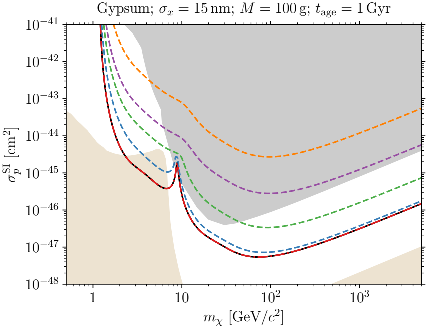

Sensitivity for different ^{238}U concentrations

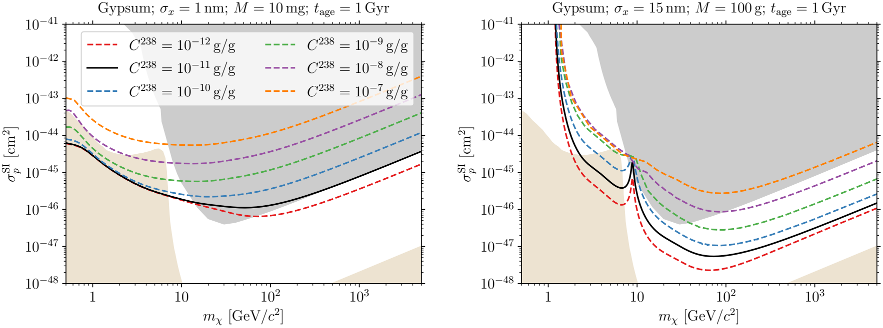

Multiple nuclei and large ϵ allow for optimal $\Delta m_X / m_X$

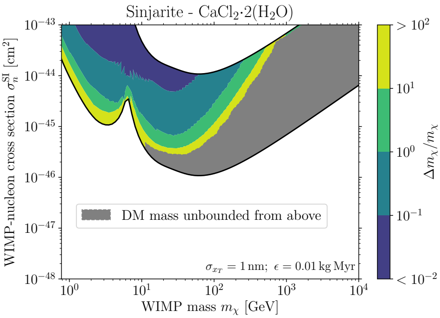

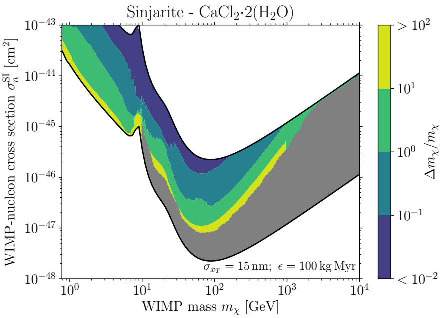

Mineral detectors can look for signals "averaged" over geological timescales or for time-varying signals

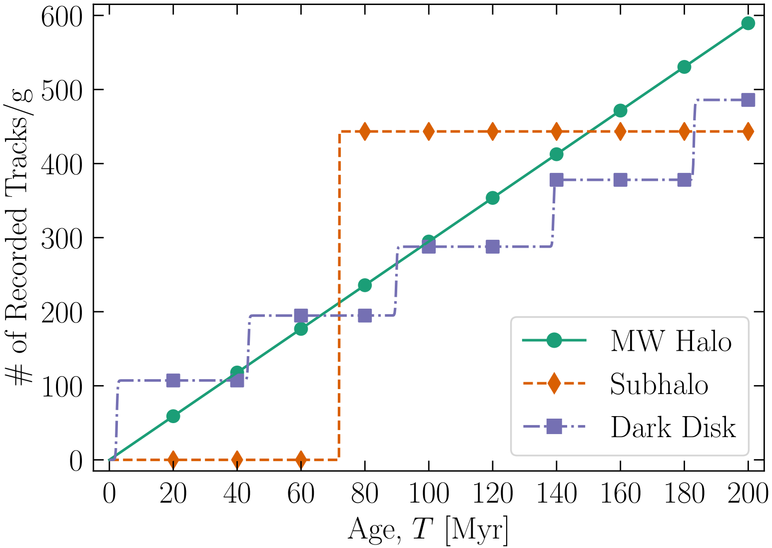

Multiple samples to detect dark disk transit every ∼ 45 Myr

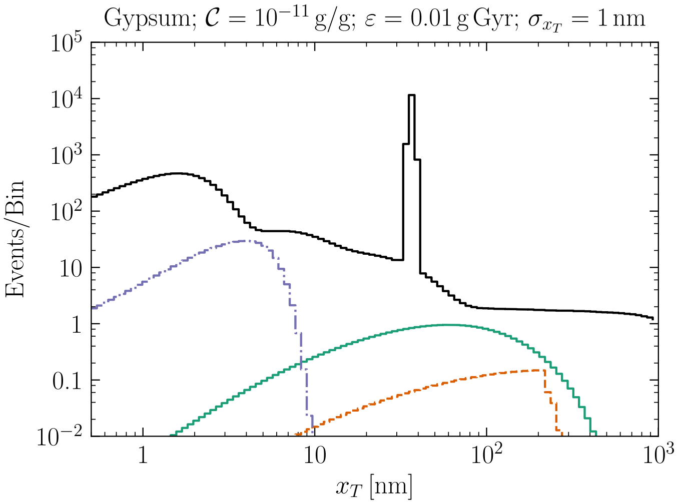

$m_X^{\rm disk} = 100$ GeV $\sigma_{Xp}^{\rm disk} = 10^{-43}\,\mathrm{cm}^2$ $m_X = 500$ GeV $\sigma_{Xp} = 5 \times 10^{-46}\,\mathrm{cm}^2$

Distinguish from halo with 20, 40, 60, 80, 100 Myr samples

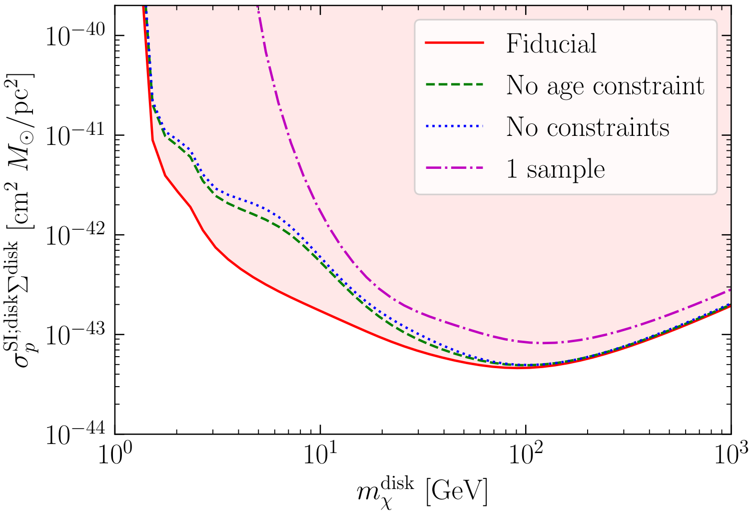

Systematic uncertainties $\Delta_t = 5\%$ $\Delta_M = 0.1\%$ $\Delta_C = 10\%$ $\Delta_\Phi = 100\%$

Change number of samples and sample spacing in time

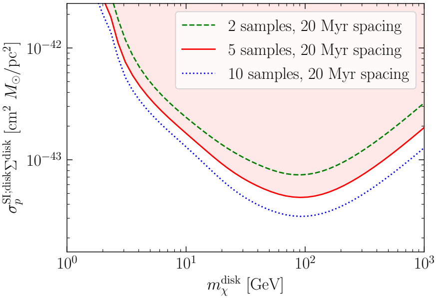

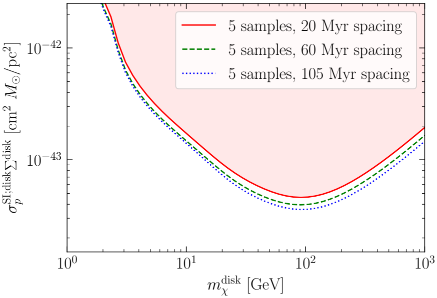

Neutrinos come from a variety of sources

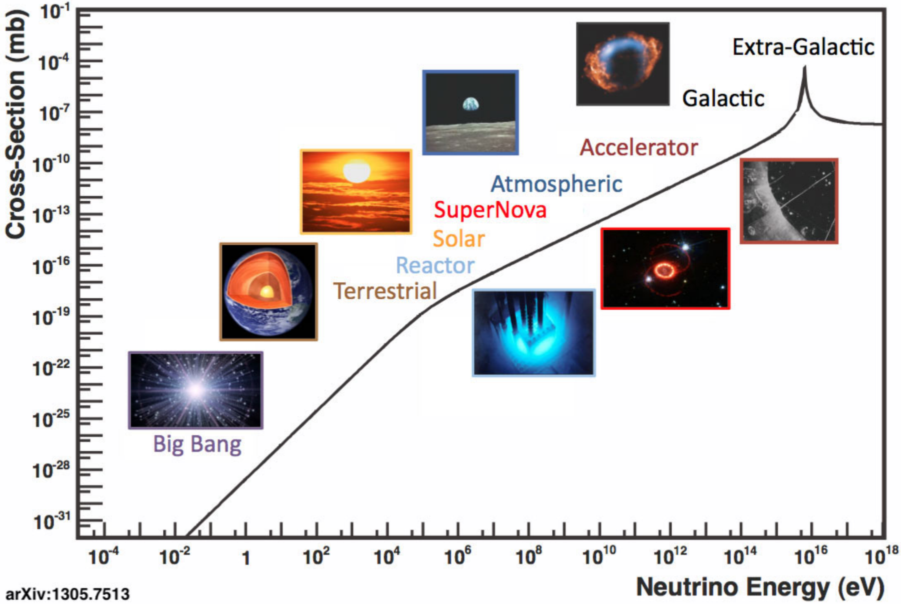

Nuclear recoil spectrum depends on neutrino energy

$$\frac{dR}{dE_R} = \frac{1}{m_T} \int dE_\nu \frac{d\sigma}{dE_R} \frac{d\phi}{dE_\nu}$$

- Quasi-elastic for $E_\nu \gtrsim 100\,\text{MeV}$
- Resonant π production at $E_\nu \sim \text{GeV}$
- Deep inelastic for $E_\nu \gtrsim 10\,\text{GeV}$

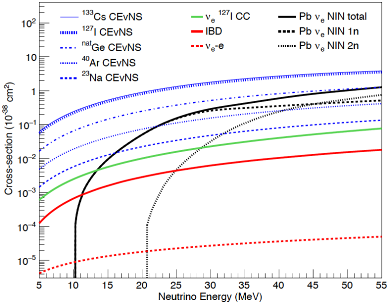

Figure: COHERENT, 1803.09183

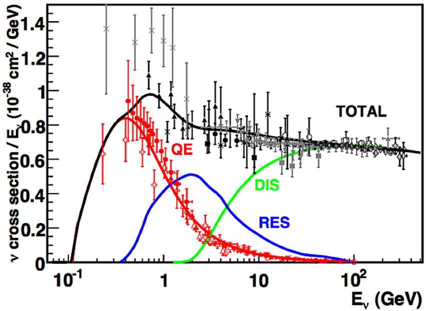

Figure: Inclusive CC $\sigma_{\nu N}$, 1305.7513

Atmospheric ν's originating from CR interactions

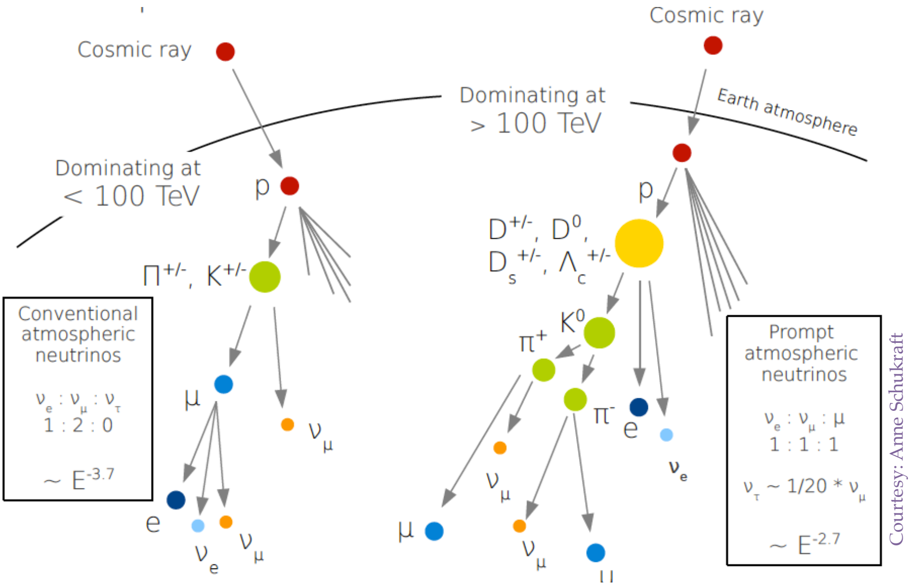

Atmospheric ν's originating from CR interactions

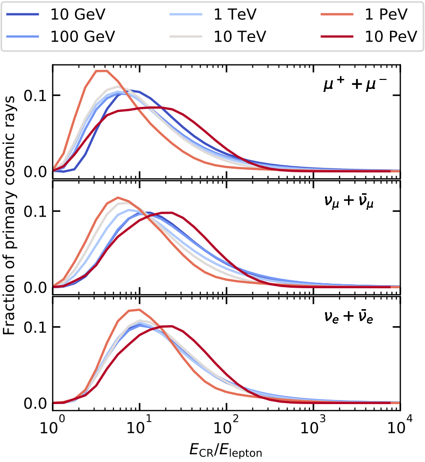

Figure: E_{CR} to leptons, 1806.04140

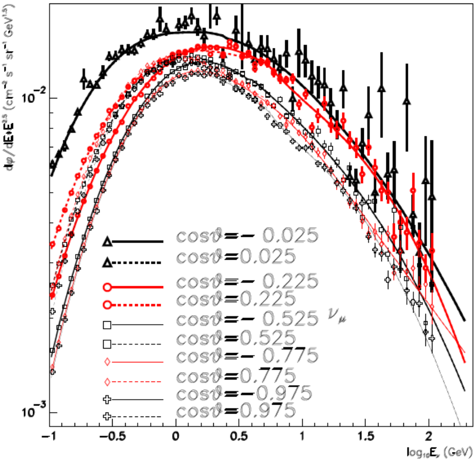

Figure: FLUKA simulation of ν_μ flux at SuperK for solar max, hep-ph/0207035

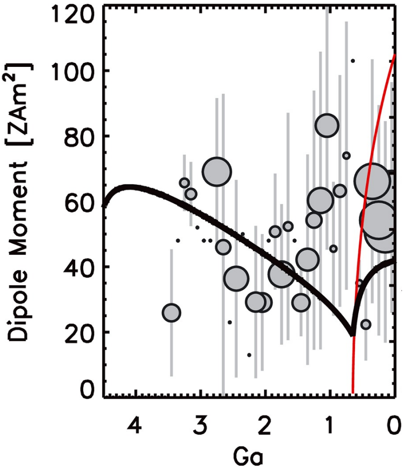

Figure: Driscoll, P. E. (2016), *Geophys. Res. Lett.*, 43, 5680-5687

Rigidity $p_{CR}/Z_{CR} \simeq E_{CR}$ for CR protons

- Rigidity cutoff $\propto M_{dip}$ truncates atmospheric ν spectrum at low E_ν
- Maximum cutoff today $\sim 50\,\mathrm{GV}$
- Recall CR primary $E_{CR} \gtrsim 10\,E_\nu$

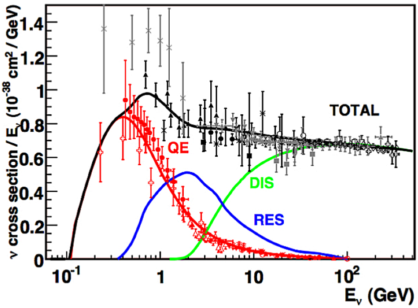

Recoil spectra from atmospheric ν's incident on NaCl(P)

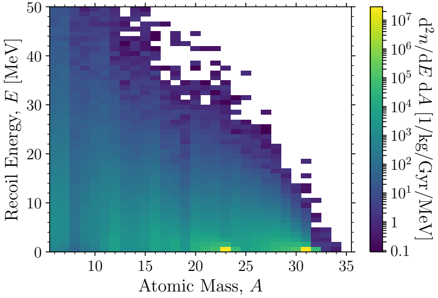

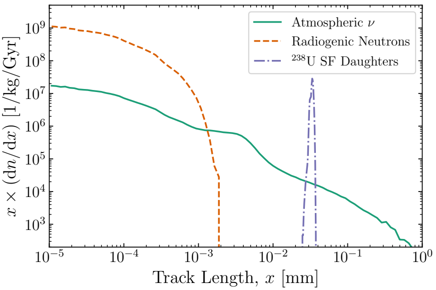

Recoils of many different nuclei

- Low energy peak from QE neutrons scattering ^{23}Na, ^{31}P
- High energy tail of lighter nuclei produced by DIS

Background free regions for $\gtrsim 1\,\mu$m

- Radiogenic n-bkg confined to low x, regardless of target
- Subdominant systematics from atmosphere, heliomagnetic field

Galactic contribution to ν flux over geological timescales

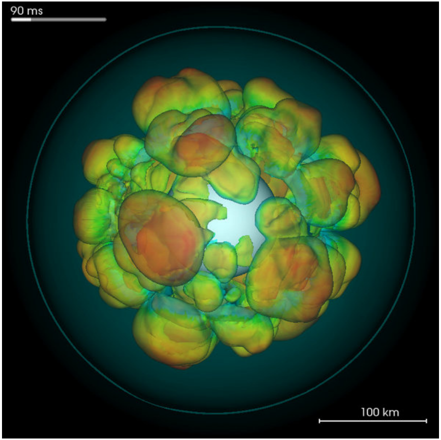

Figure: Supernova simulation after CC

Only $\sim$ 2 SN 1987A events/century

- Measure galactic CC SN rate
- Traces star formation history

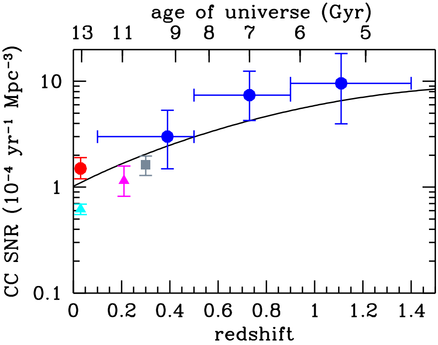

Figure: Cosmic CC SNR, 1403.0007

Galactic contribution to ν flux over geological timescales

$$\frac{d\phi}{dE_\nu} = \dot{N}_{CC}^{gal} \frac{dn}{dE_\nu} \int_0^\infty dR_E \frac{f(R_E)}{4\pi R_E^2}$$

Only $\sim$ 2 SN 1987A events/century

- Measure galactic CC SN rate
- Traces star formation history

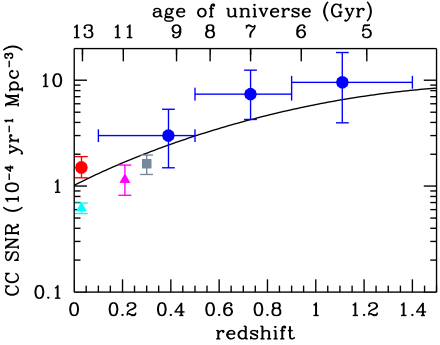

Figure: Cosmic CC SNR, 1403.0007

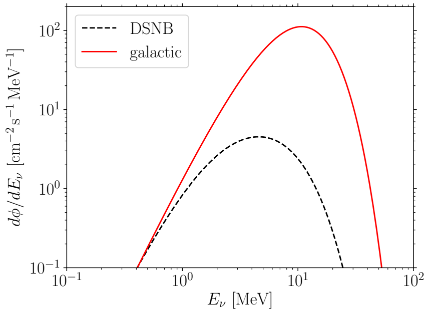

Sensitivity to galactic CC SN rate depends on C^{238}

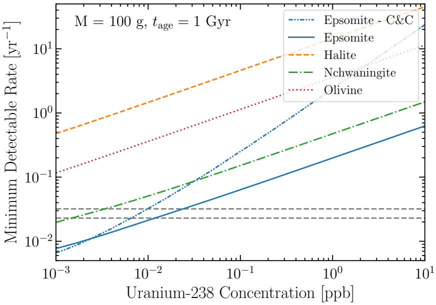

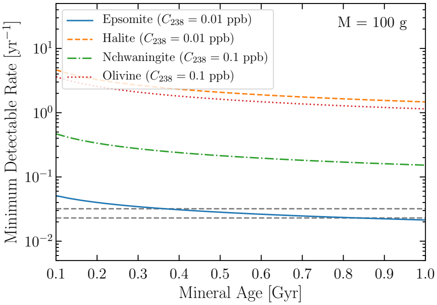

Epsomite [$Mg(SO_4)\cdot 7(H_2O)$]
Halite [NaCl]

Nchwaningite [$Mn^{2+}_2SiO_3(OH)_2\cdot(H_2O)$]
Olivine [$Mg_{1.6}Fe^{2+}_{0.4}(SiO_4)$]

Difficult to pick out time evolution of galactic CC SN rate

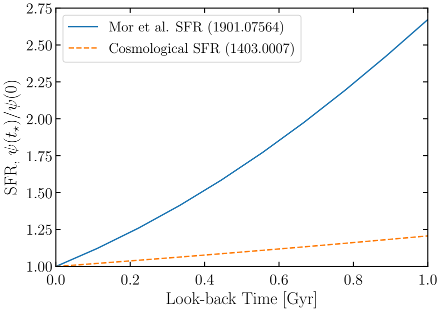

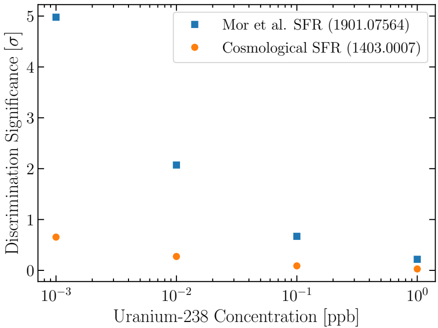

Coarse grained cumulative time bins

- 10 Epsomite paleo-detectors
- 100 g each, $\Delta t_{\rm age} \simeq 100$ Myr

Determine σ rejecting constant rate

Could only make discrimination at 3σ for $\mathcal{O}(1)$ increase in star formation rate with $C^{238} \lesssim 5$ ppt

Solar ν's produced in fusion chains from H to He

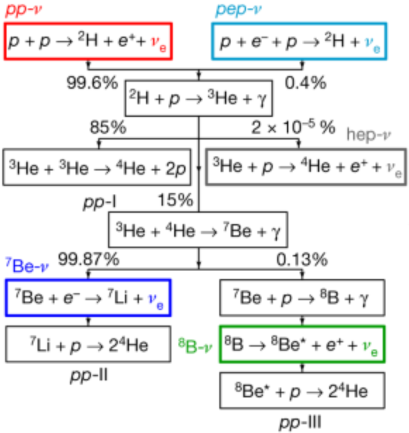

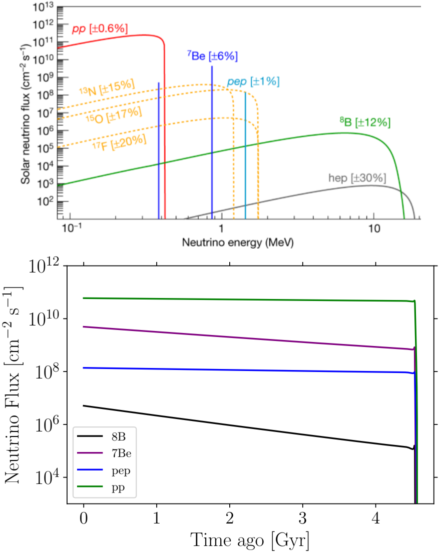

Figure: Today's flux at Borexino (Nature, 2018) and time dependence of GS metallicity model, 2102.01755

Could use large exposure to differentiate between scenarios

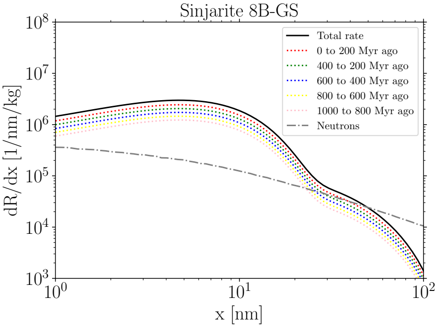

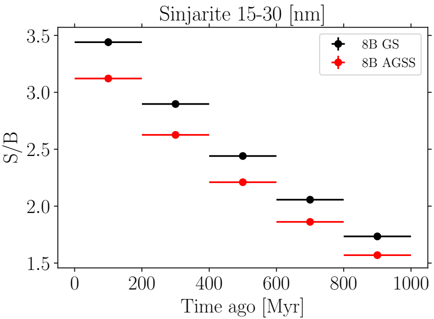

Could measure ^{8}B flux over time

- Higher $E_\nu \Rightarrow$ longer tracks
- Highly dependent on solar core temperature with flux $\propto T^{24}$
- Sensitive to metallicity model

100 g samples with 15 nm resolution

- Look in single bin $15 - 30\,\text{nm}$
- Assume $\Delta_t \sim 10\%$, $\Delta_C = 10\%$
- $N_{\text{tot}}^{\text{GS}} \sim (1.63 \pm 0.05) \times 10^6$
  $N_{\text{tot}}^{\text{AGSS}} \sim (1.52 \pm 0.05) \times 10^6$

Semi-analytic range calculations and SRIM agree with data

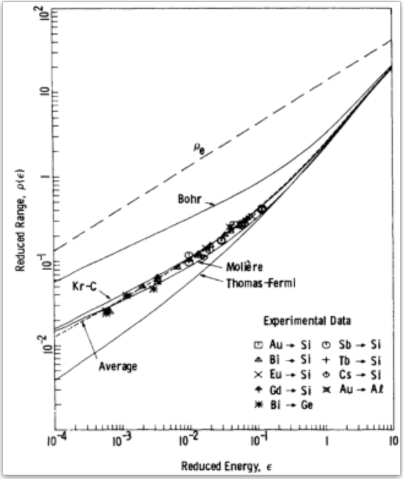

Figure: Wilson, Haggmark+ '76